3rd rencontre PhyNuBE

Structure and angular momentum at scission from microscopic models

Guillaume SCAMPS

UNIVERSITÉ TOULOUSE III PAUL SABATIER

L2IT

cnrs

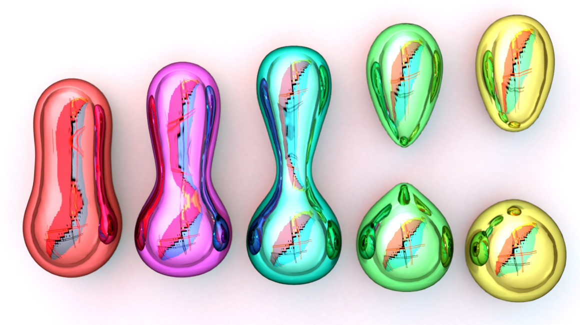

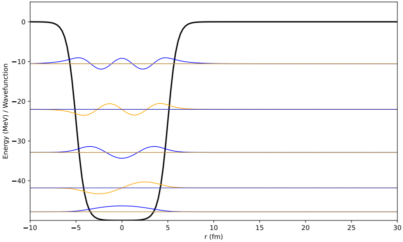

Hartree-Fock

$$\hat{h}_{MF}(\rho)\left|\varphi_i\right\rangle = \epsilon_i \left|\varphi_i\right\rangle$$

with $\hat{h}_{MF}(\rho)$ the self-consistent mean-field Hamiltonian

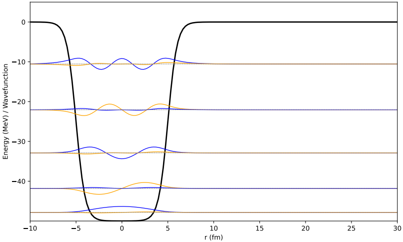

Hartree-Fock

$$\hat{h}_{MF}(\rho)\,|\varphi_i\rangle = \epsilon_i\,|\varphi_i\rangle$$

with $\hat{h}_{MF}(\rho)$ the self-consistent mean-field Hamiltonian

Time-Dependent Hartree-Fock

$$i\hbar\frac{d}{dt}|\varphi_i\rangle = (\hat{h}_{MF}(\rho) - \epsilon_i)|\varphi_i\rangle$$

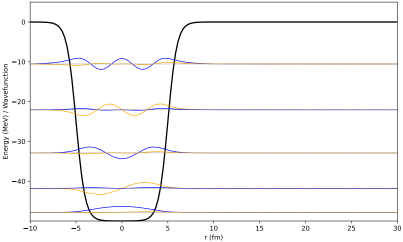

Hartree-Fock

$$\hat{h}_{MF}(\rho)\,|\varphi_i\rangle = \epsilon_i\,|\varphi_i\rangle$$

with $\hat{h}_{MF}(\rho)$ the self-consistent mean-field Hamiltonian

Time-Dependent Hartree-Fock

$$i\hbar\frac{d}{dt}|\varphi_i\rangle = (\hat{h}_{MF}(\rho) - \epsilon_i)|\varphi_i\rangle$$

Application of mean-field dynamics

Collective Mode

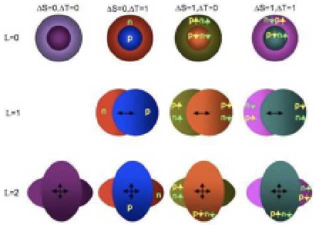

Reactions

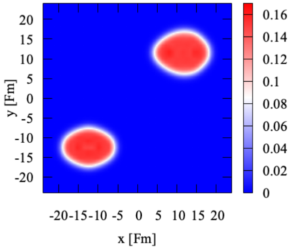

Fission

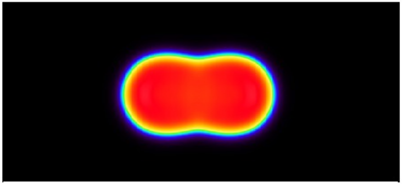

Collective Mode

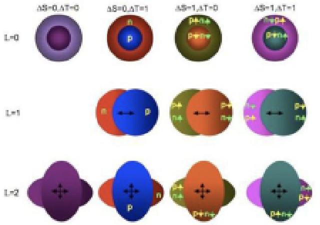

Reactions

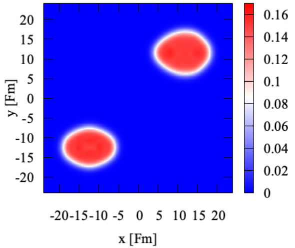

Fission

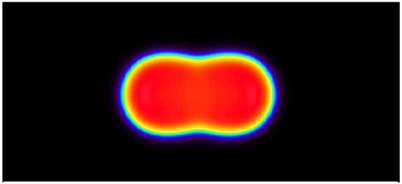

Collective Mode

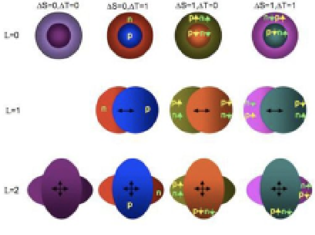

Reactions

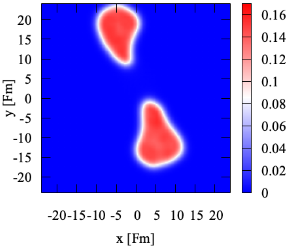

Fission

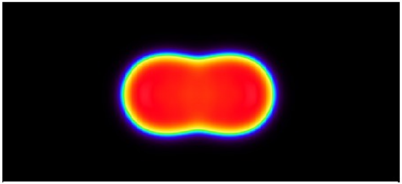

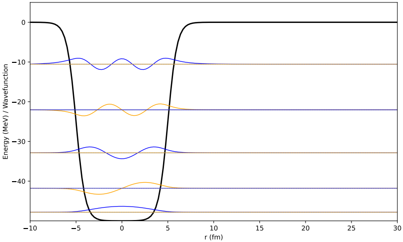

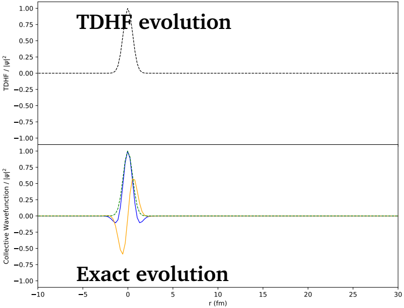

Uncertainty principle

$$\Delta X_{\mathrm{c.m.}} \Delta P_{\mathrm{c.m.}} \geq \hbar/2$$

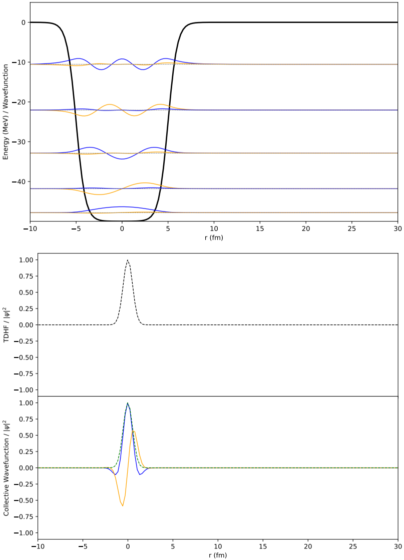

Uncertainty principle

$$\Delta X_{\mathrm{c.m.}} \Delta P_{\mathrm{c.m.}} \geq \hbar/2$$

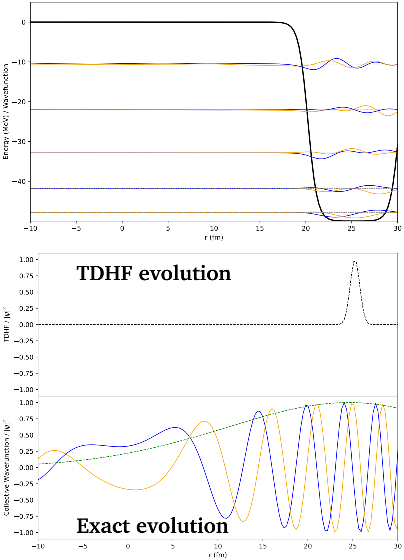

Uncertainty principle

$$\Delta X_{\text{c.m.}} \Delta P_{\text{c.m.}} \geq \hbar/2$$

Limitation of the TDHF evolution

Classical description of the collective variable

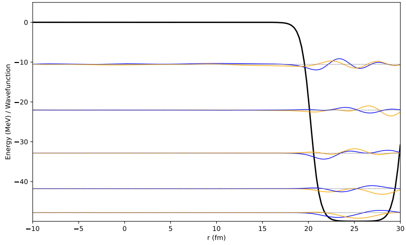

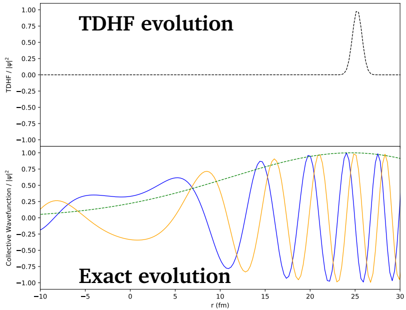

Uncertainty principle

$$\Delta X_{\text{c.m.}} \Delta P_{\text{c.m.}} \geq \hbar/2$$

Limitation of the TDHF evolution

Classical description of the collective variable

Limitation

- no tunneling
- no fluctuation of the collective observable

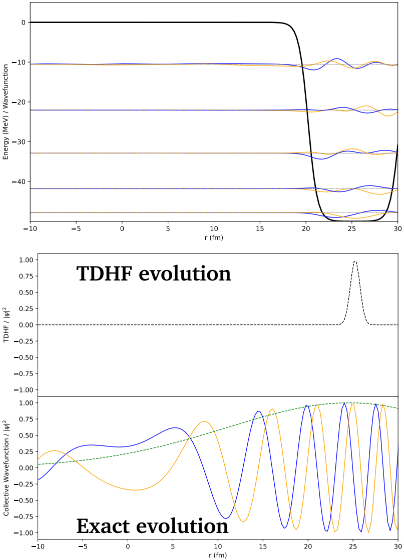

Uncertainty principle

$$\Delta X_{\mathrm{c.m.}} \Delta P_{\mathrm{c.m.}} \geq \hbar/2$$

Limitation of the TDHF evolution

Classical description of the collective variable

Limitation

- no tunneling
- no fluctuation of the collective observable

Important

The same is true with pairing (TDHF+BCS, TDHFB)

Time-dependent density functional theory - TDDFT

TDHF

- Independent particle
- Initialisation :
  $\hat{h}_{MF} |\phi_i\rangle = \epsilon_i |\phi_i\rangle$
- Evolution :
  $i\hbar \frac{d\rho}{dt} = [h_{MF}, \rho]$

TDHFB - TDSLDA

- Pairing correlation
- Quasi-particles : $|\omega_\alpha\rangle = \binom{U_\alpha}{V_\alpha}$
- One-body ρ and simplified two body density κ
- Evolution :
  $i\hbar \frac{d|\omega_\alpha\rangle}{dt} = \begin{pmatrix} h & \Delta \\ -\Delta^* & -h^* \end{pmatrix} |\omega_\alpha\rangle$

Self consistent theory - Effective Skyrme functional

Fission barrier : ^{258}Fm

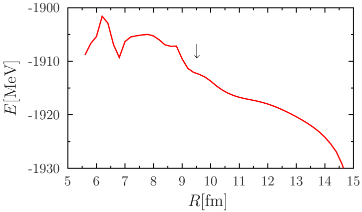

TDHF

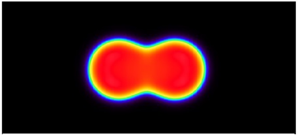

TDHF+BCS

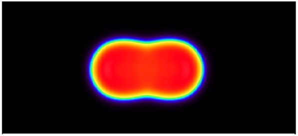

G. Scamps, C. Simenel, D. Lacroix, PRC **92**, 011602(R) (2015).

Fission barrier : ^{258}Fm

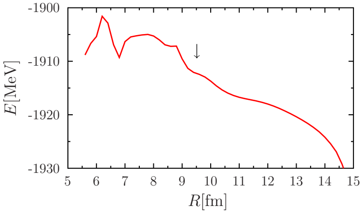

TDHF

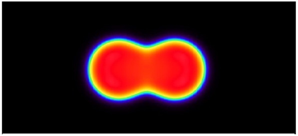

TDHF+BCS

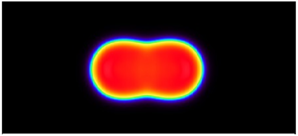

G. Scamps, C. Simenel, D. Lacroix, PRC **92**, 011602(R) (2015).

Fission barrier : ^{258}Fm

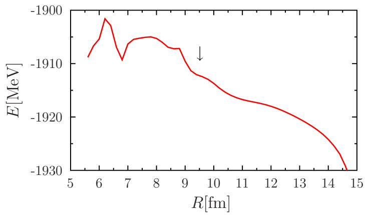

TDHF

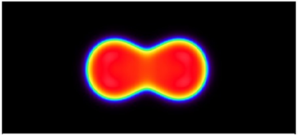

TDHF+BCS

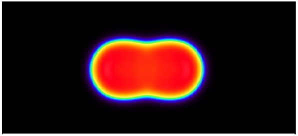

G. Scamps, C. Simenel, D. Lacroix, PRC **92**, 011602(R) (2015).

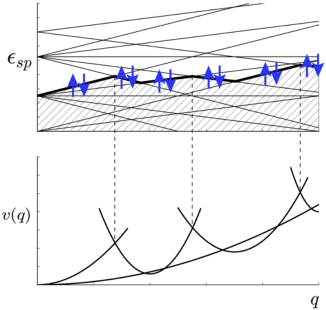

TDHF

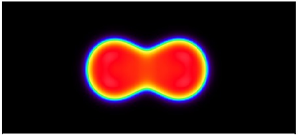

TDHF+BCS

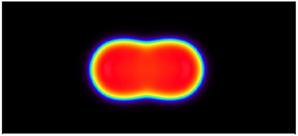

G. Scamps, C. Simenel, D. Lacroix, PRC **92**, 011602(R) (2015).

Impact of pairing

Pairing is a lubricant for fission

J. Phys. G: Nucl. Part. Phys. **47** (2020) 113002 Topical Review

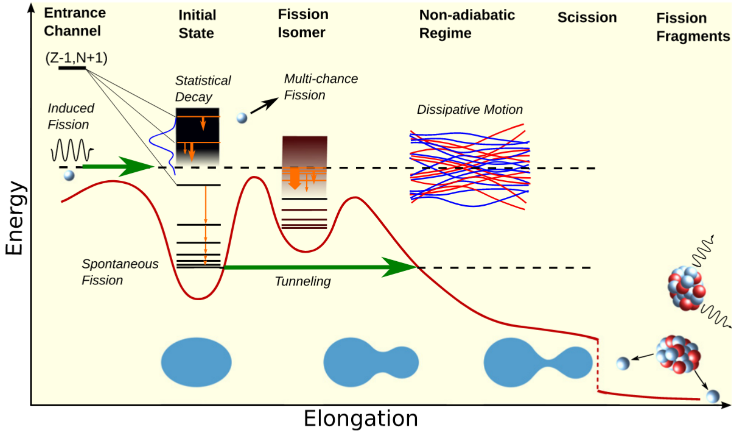

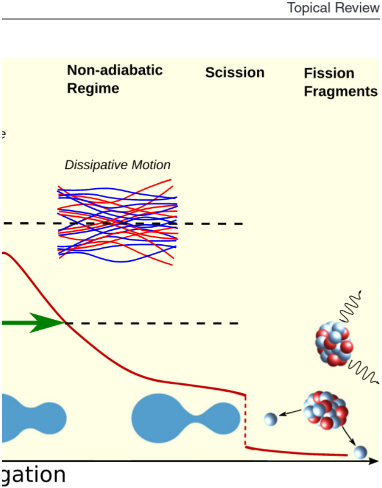
Topical Review
Non-adiabatic Regime
Scission
Fission Fragments
Dissipative Motion
gation

What do we want to understand ?

- Charge and mass distribution
- Connection with structure
- Odd-even effects
- Charge polarization
- Spin of the fragments

Topical Review

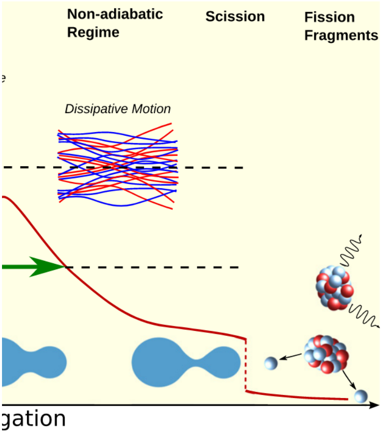

Empirical behaviour of actinide nuclei

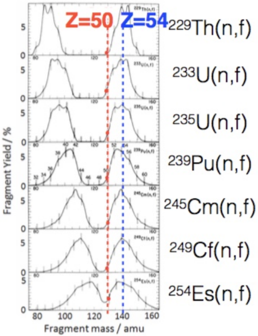

J.P. Unik, J.E. Gindler, J.E. Glendenin et al. : Proc. Phys. and Chem. of Fission IAEA Vienna, Vol II, 20 (1974)

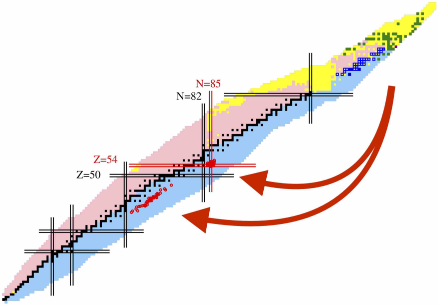

Data from D. A. Brown et al., Endf/b-viii.0, Nucl. Data Sheets 148, 1 (2018), (spontaneous and thermal neutron-capture).

Empirical behavior of actinide nuclei

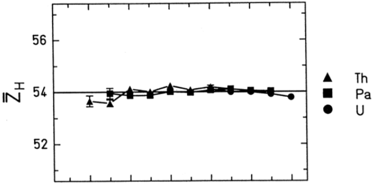

K.-H. Schmidt et al. Nuclear Physics A 665 (2000)

C. Böckstiegel et al. / Nuclear Physics A 802 (2008) 12–25

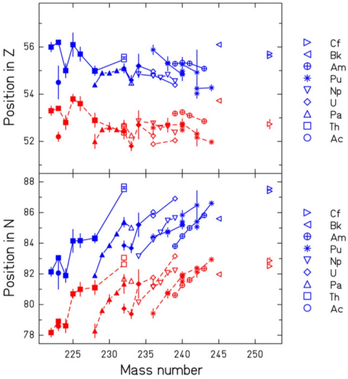

Motivation

How can we understand this behaviour ? Interplay between structure and reactions ?

First : CHF+BCS

Example : ^{240}Pu

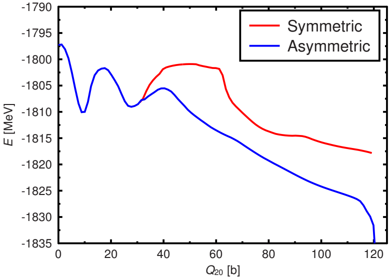

Second : TDHF+BCS

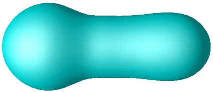

First : CHF+BCS

Example : ^{240}Pu

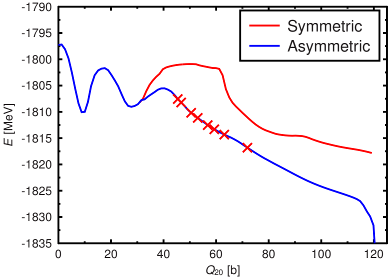

Second : TDHF+BCS

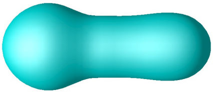

First : CHF+BCS

Example : ^{240}Pu

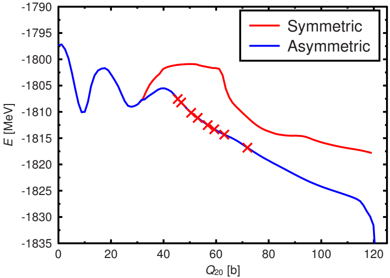

Second : TDHF+BCS

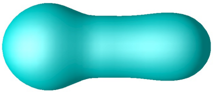

TDHF+BCS

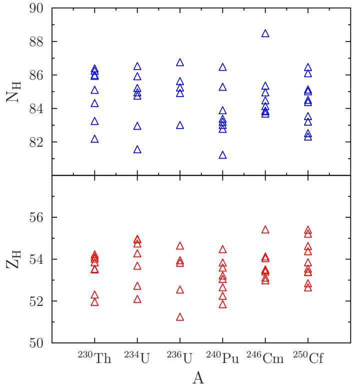

Comparison with experimental data

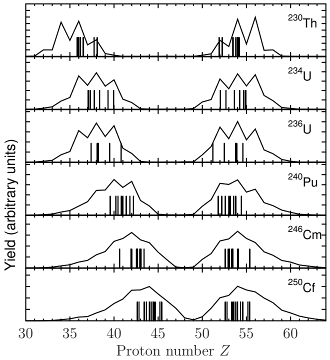

TDHF+BCS

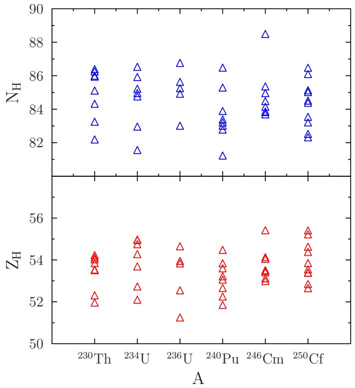

Comparison with experimental data

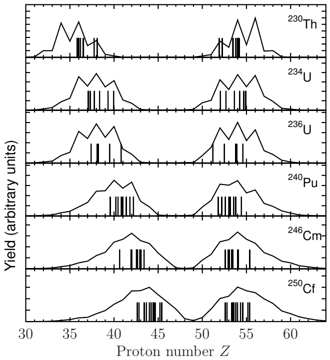

Conclusion :

The TDHF+BCS calculation reproduces well the Z=54 behavior. But why?

^{240}Pu

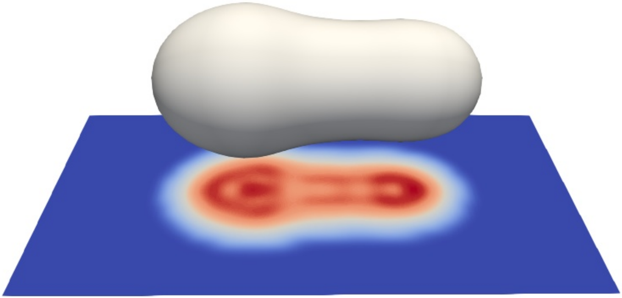

Example of ^{240}Pu

^{240}Pu

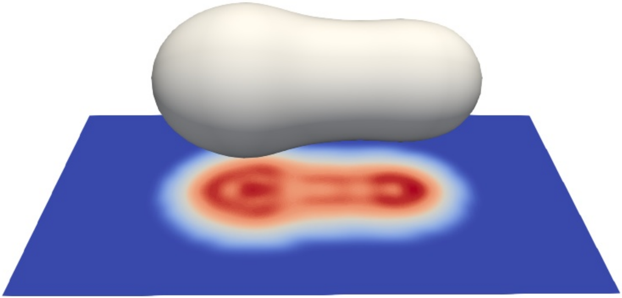

^{240}Pu

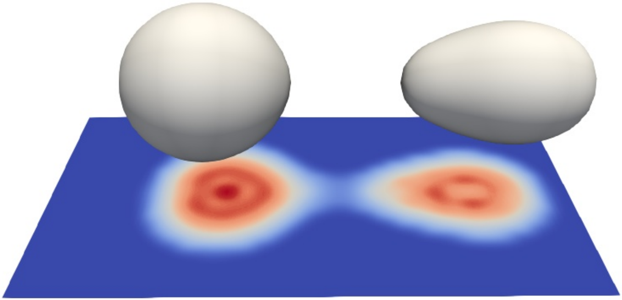

^{240}Pu

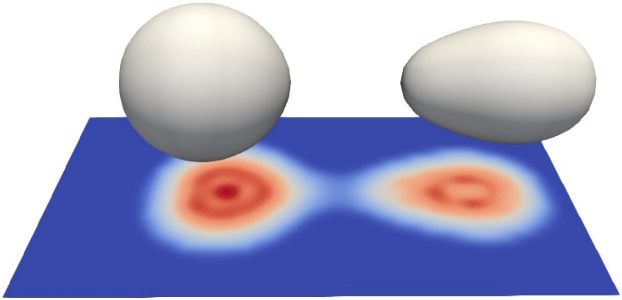

Other systems

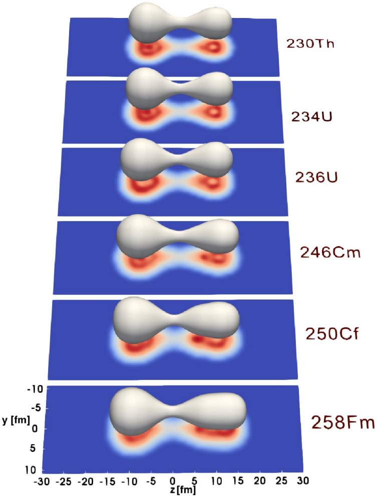

Other systems

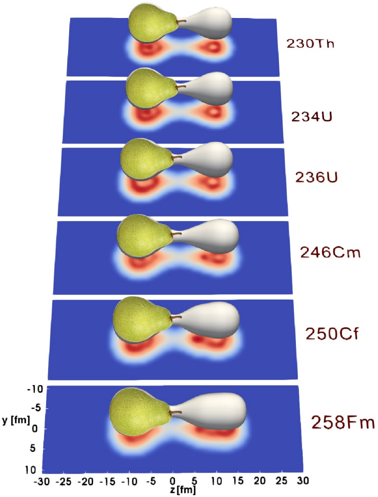

Similar effect on fusion reaction :

^{40}Ca+^{40}Ca, $E3^{-} = 3.7$ MeV

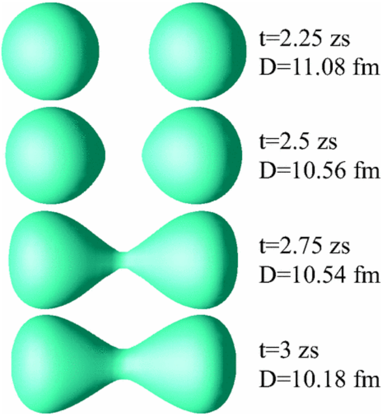

^{56}Ni+^{56}Ni, $E3^{-} = 7.5$ MeV

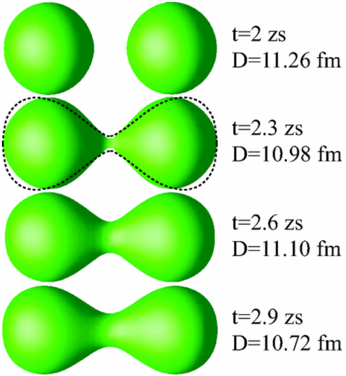

C. Simenel, M. Dasgupta, D. J. Hinde, and E. Williams, Phys. Rev. C 88, 064604 (2013).

Similar effect on fusion reaction :

^{40}Ca+^{40}Ca, $E3^-$ = 3.7 MeV

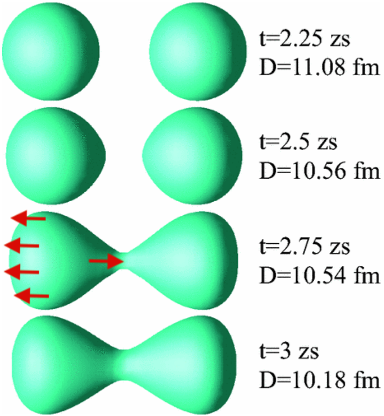

^{56}Ni+^{56}Ni, $E3^-$ = 7.5 MeV

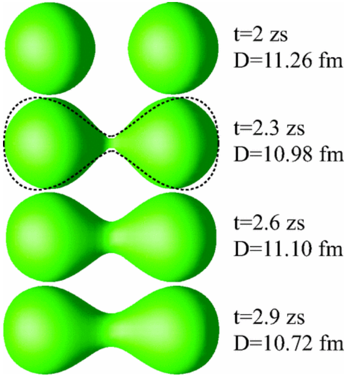

C. Simenel, M. Dasgupta, D. J. Hinde, and E. Williams, Phys. Rev. C 88, 064604 (2013).

Skyrme Skm*.

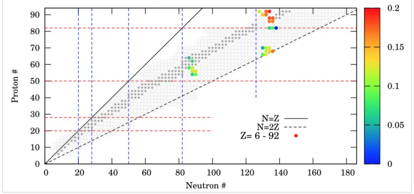

S. Ebata, and T. Nakatsukasa, Phys. Scr. 92 (2017)

Gogny D1S

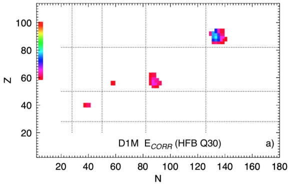

LM Robledo - J. phys. G : Nucl. and Part. Phys. (2015)

Results from systematic calculation

In both calculations, the region $Z \simeq 56$, $N \simeq 88$ is favorable for octupole deformation.

Experimental results

^{144}Ba is found to be octupole in its ground state. Burcher et al. PRL 116 (2016).

Skyrme Skm*.

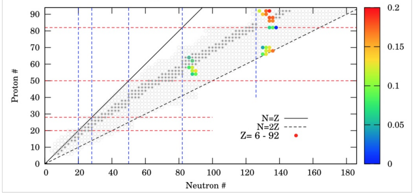

S. Ebata, and T. Nakatsukasa, Phys. Scr. 92 (2017)

Fission data

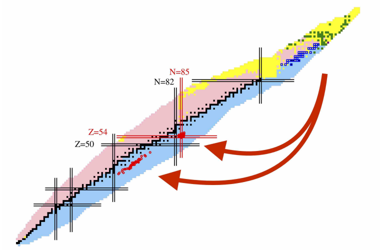

Results from systematic calculation

In both calculations, the region Z $\simeq$ 56, N $\simeq$ 88 is favorable for octupole deformation.

Experimental results

^{144}Ba is found to be octupole in its ground state. Burcher et al. PRL 116 (2016).

Structure, ^{144}Ba, Z=56, N=88

Q_2 - Q_3 potential energy surface

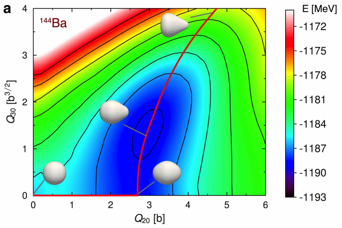

Single particle energy

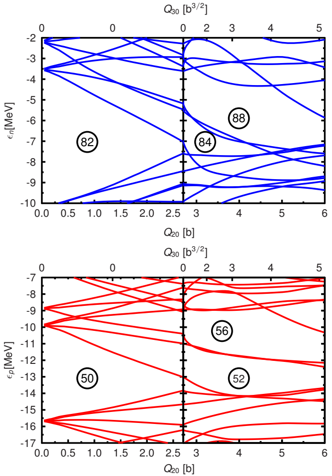

Single particle energies

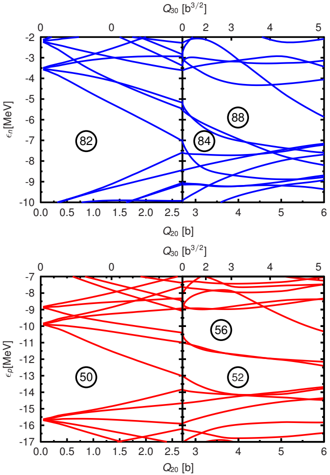

Experimental results

C. Böckstiegel et al. / Nuclear Physics A 802 (2008) 12–25

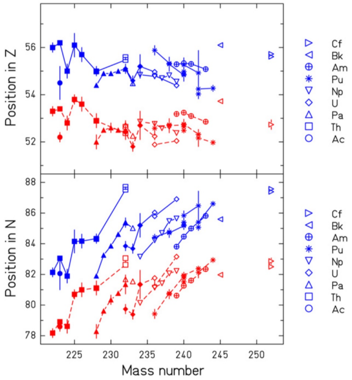

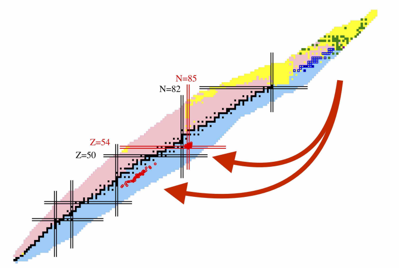

Mechanism

- The Nucleus-Nucleus interaction at the scission configuration favors the octupole shapes
- Shell structure favors octupole shape in the region Z $\simeq$ 52-56, N $\simeq$ 84-88
- Actinide fission fragments are driven in the region Z $\simeq$ 54, N $\simeq$ 86

G. Scamps, C. Simenel, Nature 564, 382 (2018).

Fission of light nuclei

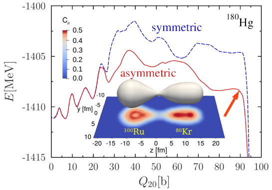

G. Scamps C. Simenel, PRC 100, 041602(R) (2019)

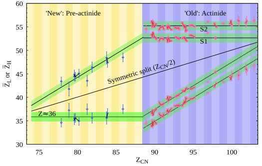

K. Mahata, C. Schmitt, S. Gupta, A. Shrivastava, G. Scamps, K.-H. Schmidt, PLB 825, 136859 (2022)

Scission point model

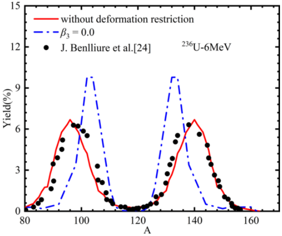

Dong-ying Huo, Zheng Wei, et al., PRC108, 024608(2023)

Quasi-fission ; Ex. $^{40-56}$Ca+^{176}Yb

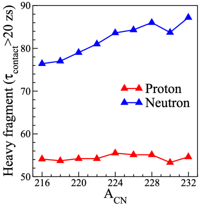

C. Simenel, et al, J.P. CS 2586(2023).

Spin of the Fragments

Spin of the fragments

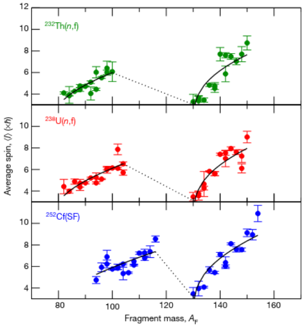

Correlations

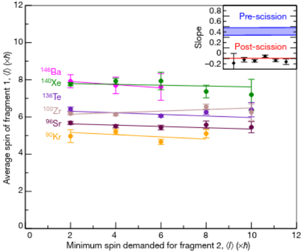

J. N. Wilson, Nature, 590, 566 (2021)

- The average spin follows a sawtooth shape
- No correlations between the spins of the fragments

Spins are mostly perpendicular to the fission axis

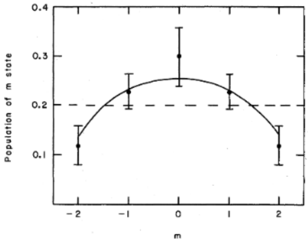

FIG. 9. The points are the calculated populations of the various m substates of the 2^+ level in ^{144}Ba. These values were determined using the fitted experimental angular distribution of the $2^+ \to 0^+$ γ ray. The solid line represents the predicted population of the m states as calculated from the statistical-model analysis of the de-excitation process using Eqs. (4) and (5) with an assumed value of $B=6$ [Eq. (3)] for the initial angular momentum distribution.

J. B. Wilhelmy, E. Cheifetz, R. C. Jared, S. G. Thompson, H. R. Bowman, and J. O. Rasmussen Phys. Rev. C 5, 2041 (1972)

What generates the fragments' spin ?

Literature

- Thermal excitations
- Quantum fluctuations
- Coulomb force
- Breaking of the neck

Tilting Mode

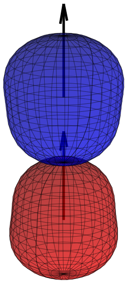

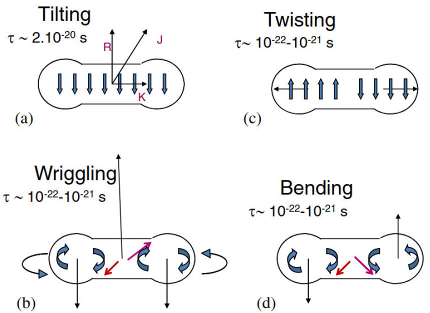

Illustration from B. John, J. Phys., 85, 2, (2015).

What generates the fragments' spin ?

Literature

- Thermal excitations
- Quantum fluctuations
- Coulomb force
- Breaking of the neck

Tilting Mode

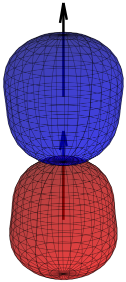

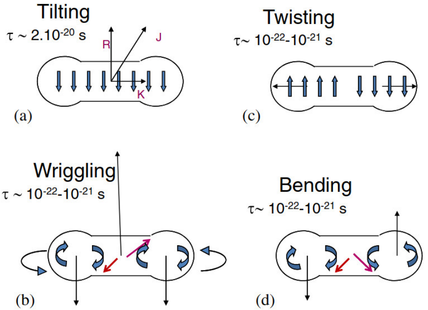

Illustration from B. John, J. Phys., 85, 2, (2015).

Literature

- Thermal excitations
- Quantum fluctuations
- Coulomb force
- Breaking of the neck

Twisting Mode

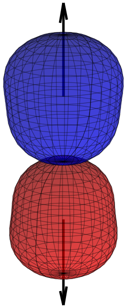

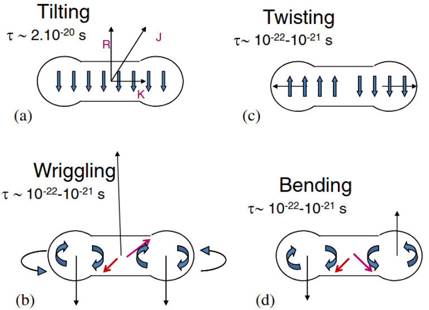

Illustration from B. John, J. Phys., 85, 2, (2015).

What generates the fragments' spin ?

Literature

- Thermal excitations
- Quantum fluctuations
- Coulomb force
- Breaking of the neck

Wriggling Mode

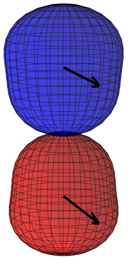

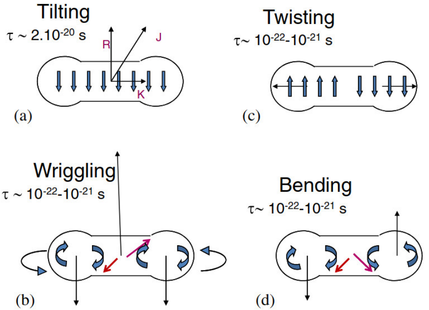

Illustration from B. John, J. Phys., 85, 2, (2015).

What generates the fragments' spin ?

Literature

- Thermal excitations
- Quantum fluctuations
- Coulomb force
- Breaking of the neck

Bending Mode

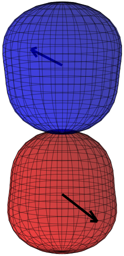

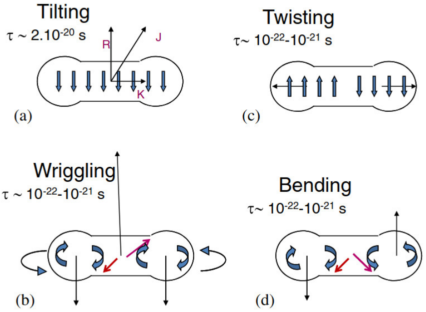

Illustration from B. John, J. Phys., 85, 2, (2015).

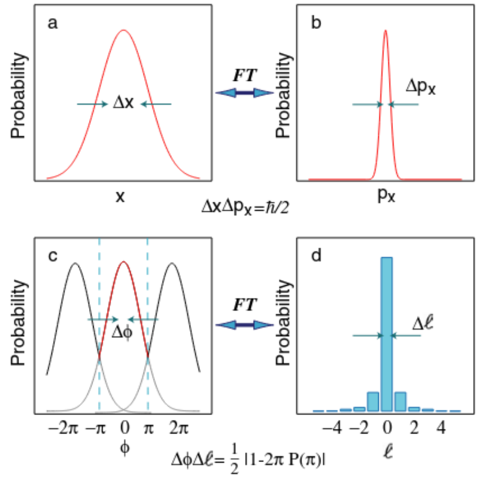

S. Franke-Arnold, et al. New Journal of Physics 6, 103 (2004)

Orientation pumping mechanism

Isotropic potential at scission

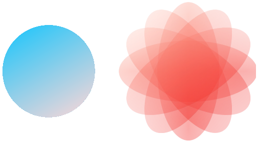

Confining potential at scission

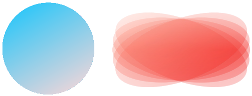

I.N Mikhailov, P Quentin, PLB 462 (1999).

Static HFB

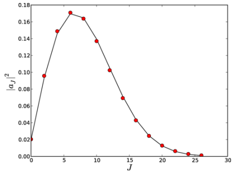

G. F. Bertsch, T. Kawano, and L. M. Robledo, PRC 99, 034603 (2019)

Scission configuration

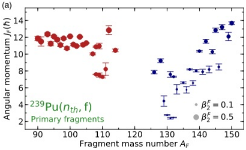

P. Marević, N. Schunck, J. Randrup, and R. Vogt PRC 104, L021601 (2021).

TDHFB - TDSLDA

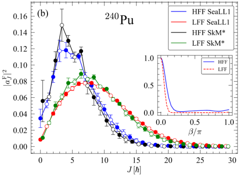

A. Bulgac, et al., PRL 126, 142502 (2021)

Projection method

$$|a_J^F|^2 = \frac{2J+1}{2}\int_0^{2\pi} \sin(\beta)\, P_J(\cos(\beta))\langle\Psi|e^{\frac{-i\hat{J}_x^F\beta}{\hbar}}|\Psi\rangle$$

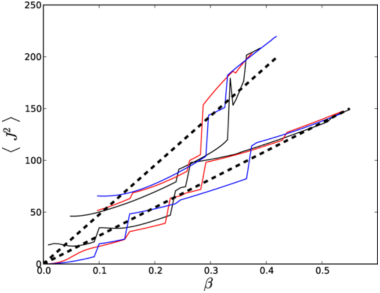

G. F. Bertsch, T. Kawano, and L. M. Robledo, PRC 99, 034603 (2019)

Problem of interpretation

- The spin cut-off distribution is already present in the ground state of even-even deformed nuclei if symmetry are not restored
- $\hat{J}^2$ and $\hat{P}(J)$ are 2 and N-body operators
- Fragments do not rotate in dynamical approaches

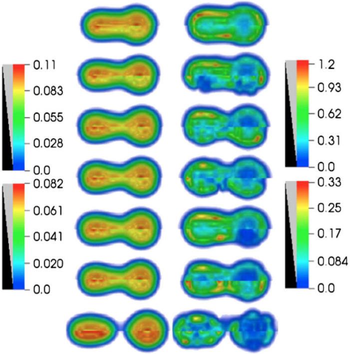

A. Bulgac, et al. PRL 116, 122504 (2016)

Problem of interpretation

- The spin cut-off distribution is already present in the ground state of even-even deformed nuclei if symmetry are not restored
- $\hat{J}^2$ and $\hat{P}(J)$ are 2 and N-body operators
- Fragments do not rotate in dynamical approaches

^{144}Ba + ^{96}Sr at 16 Fm, Θ_{ini}=25 deg, Functional : Skyrme Sly4d

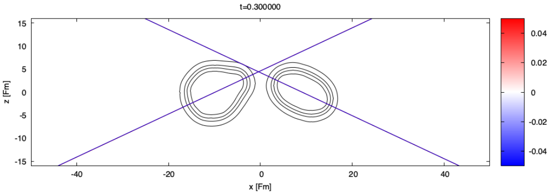

G. Scamps, PRC 106, 054614 (2022).

^{144}Ba + ^{96}Sr at 16 Fm, Θ_{ini}=25 deg, Functional : Skyrme Sly4d

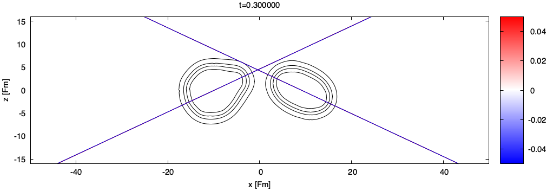

G. Scamps, PRC 106, 054614 (2022).

^{144}Ba + ^{96}Sr at 16 Fm, Θ_{ini}=25 deg, Functional : Skyrme Sly4d

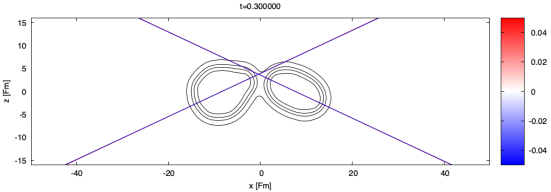

G. Scamps, PRC 106, 054614 (2022).

^{144}Ba + ^{96}Sr at 16 Fm, Θ_{ini}=25 deg, Functional : Skyrme Sly4d

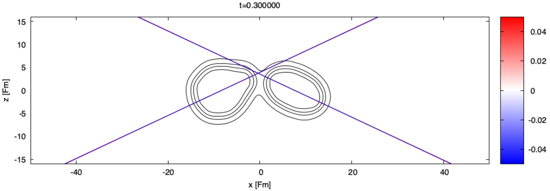

G. Scamps, PRC 106, 054614 (2022).

$^{132}Sn+^{108}Ru$

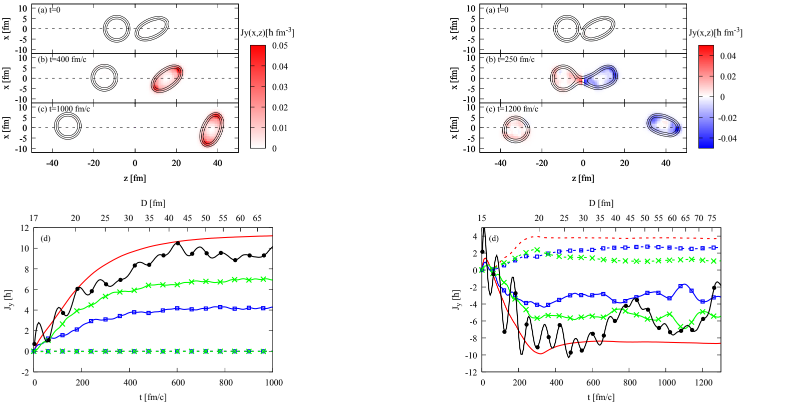

(a) t=0
(b) t=400 fm/c
(c) t=1000 fm/c
x [fm]
z [fm]
Jy(x,z)[ħ fm^-3]
(b) t=250 fm/c
(c) t=1200 fm/c
D [fm]
(d)
J_y [ħ]
t [fm/c]

^{144}Ba+^{96}Sr

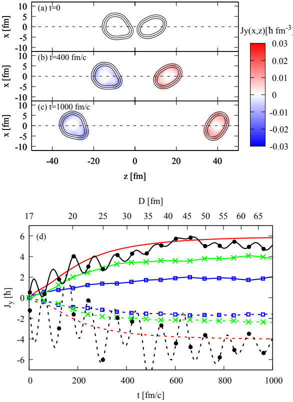
(a) t=0
(b) t=400 fm/c
(c) t=1000 fm/c
x [fm]
z [fm]
Jy(x,z)[ħ fm^-3]
(d)
D [fm]
J_y [ħ]
t [fm/c]

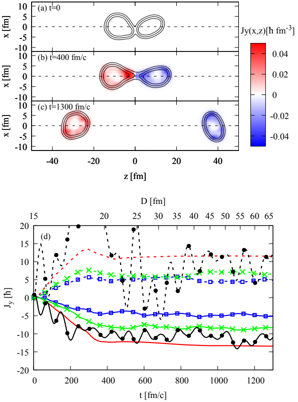
(a) t=0
(b) t=400 fm/c
(c) t=1300 fm/c
x [fm]
z [fm]
Jy(x,z)[ħ fm^-3]
(d)
D [fm]
J_y [ħ]
t [fm/c]

Potential as a function of the light fragment angle

$^{132}Sn+^{108}Ru$

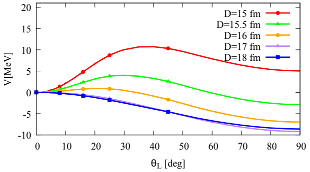

Two torques :

- attractive nucleus-nucleus torque
- repulsive Coulomb torque

Potential as a function of the light fragment angle

$^{144}Ba+^{96}Sr$. D=15.5 and 20 fm

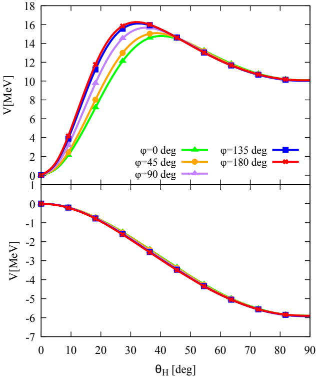

The azimuthal angle doesn't have an important role.

Method

- One body-evolution - One body-observable
- Breaking of the axial symmetry at scission

Results

- Agreement between the dynamic and the FHF potential
- Repulsive Coulomb torque ; attractive NN torque
- Small effect of the azimuthal angle

Limitation

- Classical evolution
- No prescription for the initial angle
- Frozen Hartree-Fock approximation for the initial pre-fragment

Frozen Hartree-Fock potential

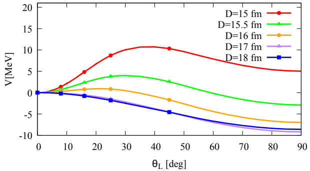

Two torques :

- attractive nucleus-nucleus torque
- repulsive Coulomb torque

4 degrees of freedom

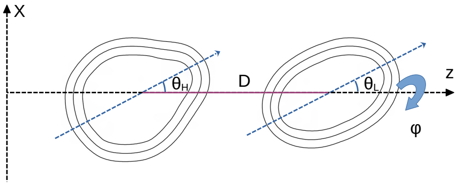

Hamiltonian

$$\hat{H}(D) = \frac{\hbar^2}{2I_H}\hat{L}_H^2 + \frac{\hbar^2}{2I_L}\hat{L}_L^2 + \frac{\hbar^2}{2I_\Lambda(D)}\hat{\Lambda}^2 + \hat{V}(\hat{\Theta}_H, \hat{\Theta}_L, \hat{\varphi}, D)$$

Solved in basis $|L_H, m, L_L, -m\rangle$

G. Scamps, G. Bertsch, Phys. Rev. C 108, 034616(2023).
Similar to the orientation pumping mechanism model Mikhailov, I. N., and Quentin, P. (1999). On the spin of fission fragments, an orientation pumping mechanism. Physics Letters B, 462(1-2), 7-13.

Evolution of a one-angle wave packet assuming spherical ^{132}Sn

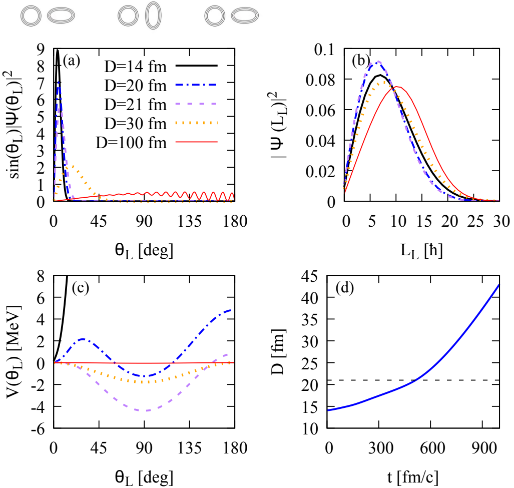

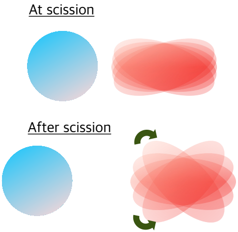

G. Scamps, G. Bertsch, Phys. Rev. C 108, 034616 (2023).

Effect of Coulomb

Effect of quadrupole deformation >> effect of $Z_1 Z_2$

TABLE II. Average spin$\langle L^2 \rangle^{\frac{1}{2}}$ in unit of $\hbar$ for the three fission fragments at scission ($D = 21$ fm) and at large distances. The last two columns show the same quantity with an MOI divided by 2.

Nucleus	Scission	Final	Scission ($I_{\frac{1}{2}}$)	Final ($I_{\frac{1}{2}}$)
^{108}Ru	9.28	12.31	7.24	10.38
^{144}Ba	10.04	10.95	7.70	8.66
^{96}Sr	7.74	9.30	6.03	7.62

also J. Randrup, PRC 108, 064606 (2023) : increase of 1 to 3 $\hbar$ due to the Coulomb torque.

Cold fission selection TXE<8MeV

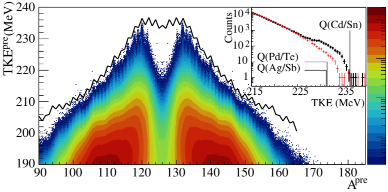

γ-spectrum

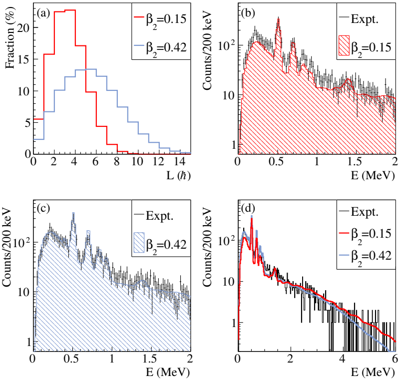

Results

- ^{132}Sn is found in ground-state
- The collective Hamiltonian model with $\beta_2=0.42$ reproduces the experimental γ-spectrum

A. Francheteau, L. Gaudefroy, G. Scamps, O. Roig, V. Méot, A. Ebran, and G. Bélier, PRL 132, 142501 (2024).

Correlation between the angular momentum

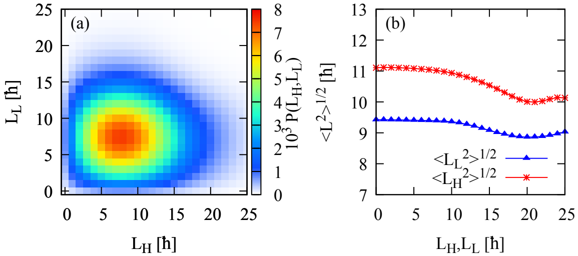

$^{144}Ba+^{96}Sr$

- No or small correlation observed in the magnitude of the angular momentum.
- More angular momentum for the heavy fragment

Effect of octupole deformation

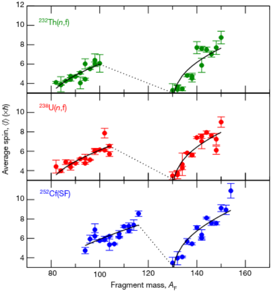

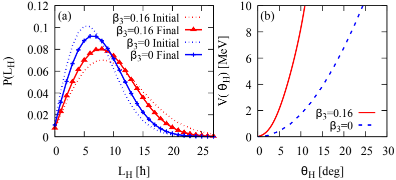

G. Scamps, G. Bertsch, Phys. Rev. C 108, 034616 (2023).

Discussion

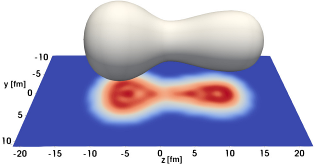

- Pear-shaped deformation plays an important role at scission. G. Scamps C. Simenel, Nature 564, pages 382–385 (2018)
- Octupole deformation makes the angular potential stiffer which increase the zero-point motion → more angular momentum

Orbital angular momemtum

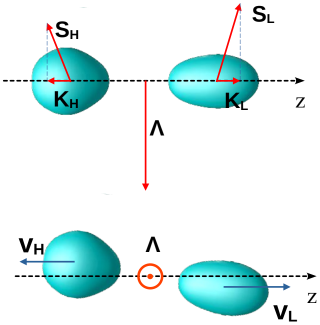

In spontaneous fission of a 0^+ state

$$\mathbf{S_H} + \mathbf{S_L} + \mathbf{\Lambda} = \mathbf{0},$$

Triangular rule :

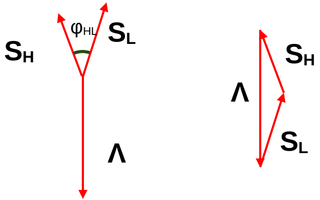

$$\cos(\varphi_{HL}) = \left(\frac{\Lambda(\Lambda+1) - S_H(S_H+1) - S_L(S_L+1)}{2\sqrt{S_H(S_H+1)S_L(S_L+1)}} \right)$$

TDDFT (in 2022) vs Freya

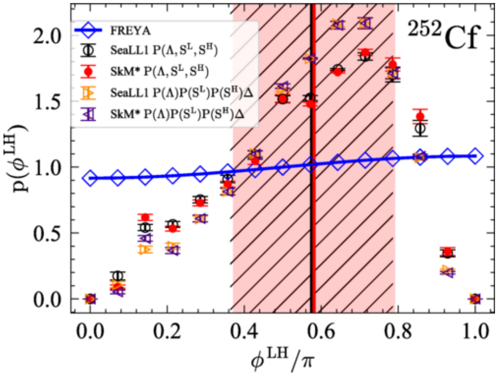

A. Bulgac, I. Abdurrahman, K. Godbey, and I. Stetcu, Phys. Rev. Lett. 128, 022501(2022).

Evolution of a three-angle wave packet

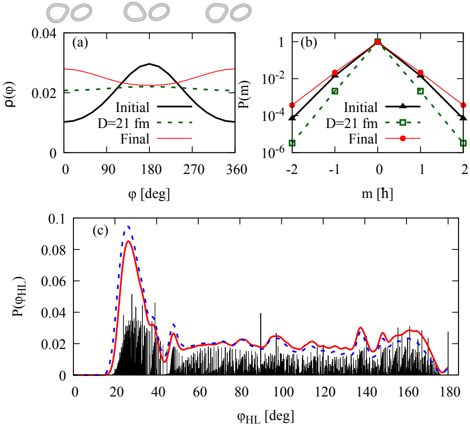

G. Scamps, G. Bertsch, Phys. Rev. C 108, 034616 (2023).

Geometry

- Small azimuthal correlation
- Spin are perpendicular to the fission axis
- Complex pattern in the opening angle, different from previous model
- Slightly more wriggling mode than bending because wriggling potential is more rigid

What do we learn from the collective hamiltonian model ?

Method

- Quantal collective model $\rightarrow$ beyond one-body
- Time-dependent evolution of a wave-packet
- Microscopic potential with FHF

Results

- No strong correlation of the magnitude and direction of the spins
- Both spins are oriented in the plane perpendicular to the fission axis.
- The Coulomb interaction induces an increase of the angular momentum by 1 to 3 $\hbar$
- The octupole deformation increases the angular momentum generated at scission

Limitation

- Frozen approximation
- Initial conditions

G. Scamps, G. Bertsch, Phys. Rev. C 108, 034616 (2023).

Projection method

Projection on the spin and K number (Projection of the spin on the fission axis)

$$\hat{P}^{S}_{MK} = \frac{(2S+1)}{16\pi^2} \int d\Omega \mathcal{D}^{S*}_{MK}(\Omega)\, e^{i\alpha \hat{S}_z} e^{i\beta \hat{S}_y} e^{i\gamma \hat{S}_z},$$

$$P(S_F, K_F) = \langle \Psi | \hat{P}^{S_F}_{K_F K_F} | \Psi \rangle,$$

Calculation of the overlap : G. F. Bertsch and L. M. Robledo, PRL 108, 042505 (2012)

$$\langle \Psi | \hat{R} | \Psi \rangle = \frac{(-1)^n}{\prod_\alpha^n v_\alpha^2} \mathrm{pf} \begin{bmatrix} V^T U & V^T R^T V^* \\ -V^\dagger R V & U^\dagger V^* \end{bmatrix}$$

Optimized Pfaffian calculation : M. Wimmer, ACM Trans. Math Softw. 38, 30 (2012).

Pair breaking mechanism ?

Spin distribution in the fragments

Obtained using 3-angle projection operator

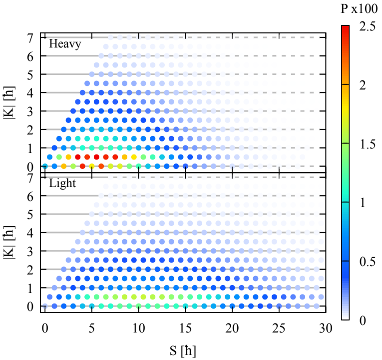

Geometry of the reaction

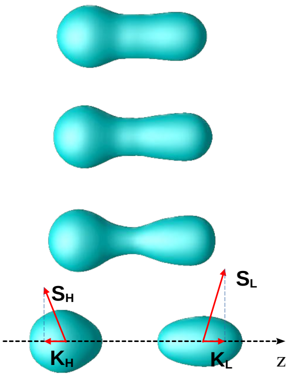

G.scamps, I. Abdurrahman, M. Kafker, A. Bulgac, and I. Stetcu, PRC 108 (6), L061602

Pair breaking mechanism ?

Assuming Cold fission

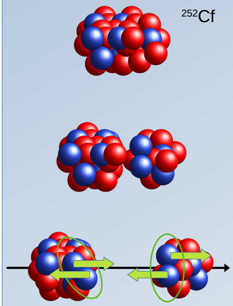

$K_H=0$ $K_L=0$

Fully paired fragments
Only even-even fragments

Realistic case

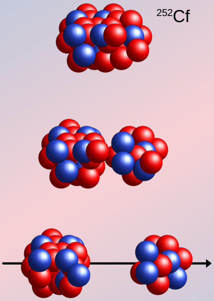

$K_H \neq 0$ $K_L \neq 0$

Pairs are broken
Every outcome are possible

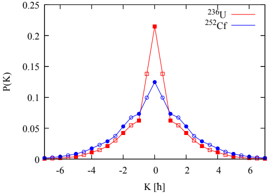

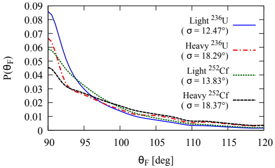

$$\cos\theta_F = \frac{K_F}{\sqrt{S_F(S_F+1)}}$$

G.scamps, I. Abdurrahman, M. Kafker, A. Bulgac, and I. Stetcu, PRC 108 (6), L061602.

$$\varphi_{HL} = \arccos\left(\frac{\Lambda(\Lambda+1) - S_H(S_H+1) - S_L(S_L+1)}{2\sqrt{S_H(S_H+1)S_L(S_L+1)}}\right)$$

$$P(\Lambda, S_H, S_L) = \sum_{k_H k_L} \langle\Psi|\hat{P}^{\Lambda}_{0,0}\hat{P}^{S_H}_{K_H K_H}\hat{P}^{S_L}_{K_L K_L}|\Psi\rangle.$$

$$P(\Lambda, S_H, S_L) = \sum_{K_H K_L K_H' K_L'} (-1)^{K_H' - K_H + K_L' - K_L}$$

$$C^{\Lambda,0}_{S_H,-K_H,S_L,-K_L} C^{\Lambda,0}_{S_H,-K_H',S_L,-K_L'} \langle\Psi|\hat{P}^{S_H}_{K_H K_H'}\hat{P}^{S_L}_{K_L K_L'}|\Psi\rangle$$

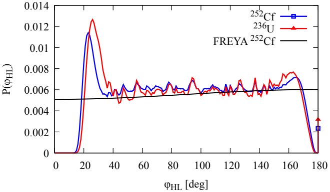

G.scamps, I. Abdurrahman, M. Kafker, A. Bulgac, and I. Stetcu, PRC 108 (6), L061602.

One angle projector :

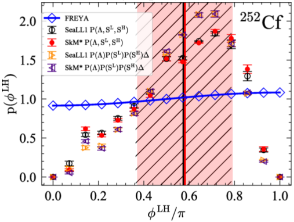

Method

- TDHFB - TDSLDA
- Full projection beyond one-angle approximation

Results

- Distribution of K
- Small fluctuations around the 90 degrees angle
- Almost flat distribution of opening angle

Limitation

- No collective wave function

G. Scamps, G. Bertsch, Phys. Rev. C 108, 034616 (2023).

Opening angle distribution

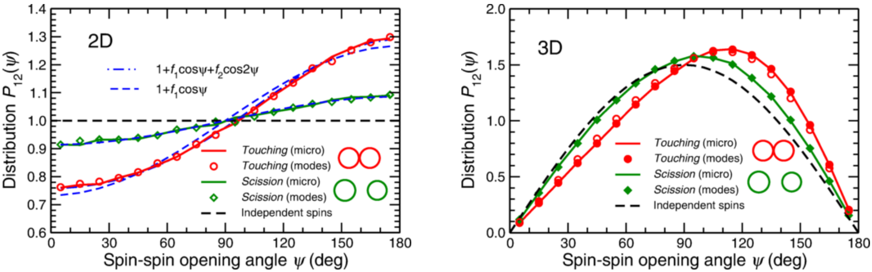

J. Randrup, Phys. Rev. C 106, L051601 (2022).

Question

- How the quantal effects change this picture ?
- How the geometry change the opening angle distribution assuming no correlation ?

Non alignement of the spins

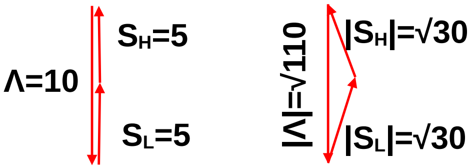

To get a 5 degrees angle between two spins require spins of 262 $\hbar$ and 6565 $\hbar$ for 1 degree

Opening angle distribution - 2D case

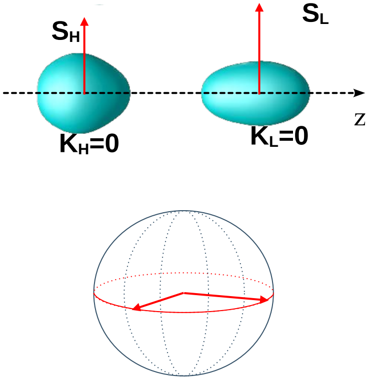

$$|\Psi\rangle = \sum_{S_H,K_H,S_L,K_L} c_{S_H,K_H,S_L,K_L} |S_H, K_H, S_L, K_L\rangle,$$

$$|c_{S_H,K_H,S_L,K_L}|^2 \propto \delta_{K_H,0}\delta_{K_L,0}(2S_H+1)e^{\frac{-S_H(S_H+1)}{2\sigma_H^2}} \times (2S_L+1)e^{\frac{-S_L(S_L+1)}{2\sigma_L^2}}.$$

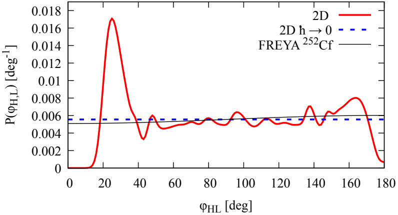

G. Scamps, PRC 109, L011602 (2024).

Opening angle distribution - 3D uniform case

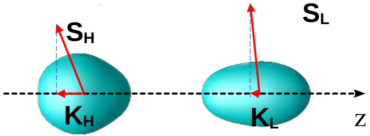

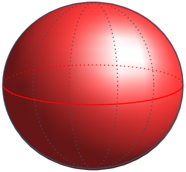

$$|\Psi\rangle = \sum_{S_H,K_H,S_L,K_L} c_{S_H,K_H,S_L,K_L} |S_H, K_H, S_L, K_L\rangle,$$

$$|c_{S_H,K_H,S_L,K_L}|^2 \propto e^{\frac{-S_H(S_H+1)}{2\sigma_H^2}} e^{\frac{-S_L(S_L+1)}{2\sigma_L^2}}.$$

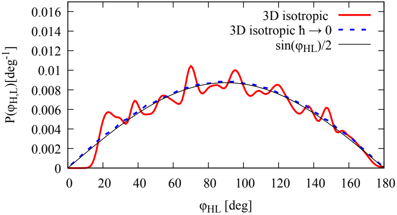

G. Scamps, PRC 109, L011602 (2024).

Opening angle distribution - 3D with total spin S=0

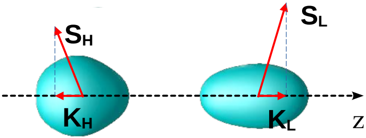

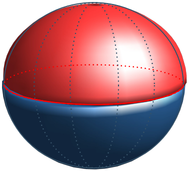

$$|\Psi\rangle = \sum_{S_H, K_H, S_L, K_L} c_{S_H, K_H, S_L, K_L} |S_H, K_H, S_L, K_L\rangle,$$

$$|c_{S_H, K_H, S_L, K_L}|^2 \propto \delta_{K_H - K_L} e^{\frac{-S_H(S_H+1)}{2\sigma_H^2}} e^{\frac{-S_L(S_L+1)}{2\sigma_L^2}}.$$

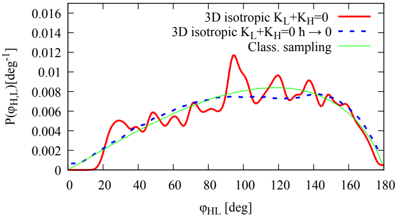

G. Scamps, PRC 109, L011602 (2024).

Opening angle distribution - 3D from TDDFT

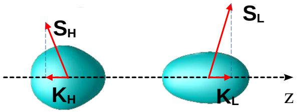

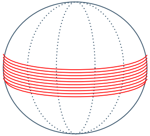

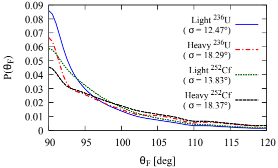

$$|\Psi\rangle = \sum_{S_H,K_H,S_L,K_L} c_{S_H,K_H,S_L,K_L} |S_H, K_H, S_L, K_L\rangle,$$

$|c_{S_H,K_H,S_L,K_L}|^2$ From TDDFT

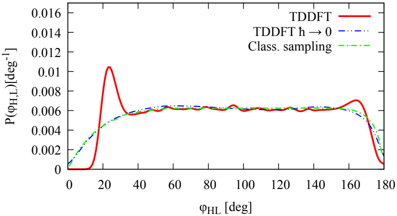

TDDFT shows an intermediate case between 2D and 3D.
G. Scamps, PRC 109, L011602 (2024).

Main points

- Orientation-pumping (uncertainty principle) mechanism at scission
- Additional effect of the Coulomb torque
- Internal excitation (breaking of pairs)
- Spins are mainly perpendicular to the fission axis
- Uncorrelated magnitude and orientation of the spins
- Dependence of the mechanism with the deformation (quadrupole and octupole)

Outlook : Case where total spin is not zero

^{208}Pb+^{208}Pb

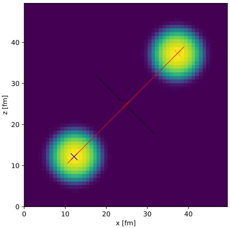

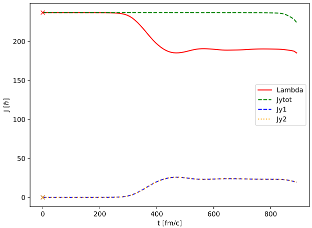

^{50}Ca+^{176}Yb

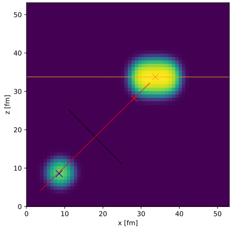

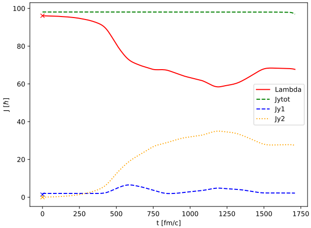

G. Scamps, Microscopic Study of Spin Transfer in Near-Barrier Nuclear Reactions, arXiv :2409.15018 (2024).

$^{208}Pb + ^{208}Pb$

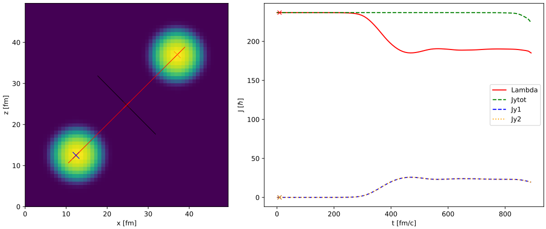

$^{50}Ca + ^{176}Yb$

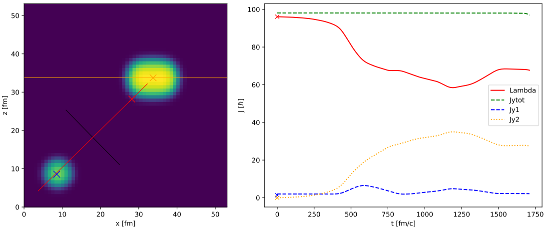

G. Scamps, Microscopic Study of Spin Transfer in Near-Barrier Nuclear Reactions, arXiv :2409.15018 (2024).

Outlook : Case where total spin is not zero

$^{208}Pb+^{208}Pb$

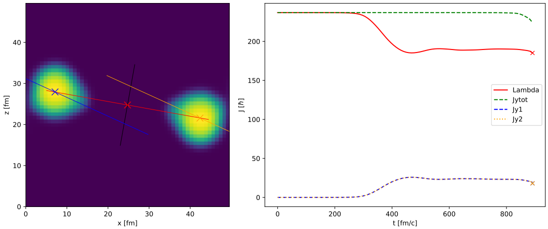

$^{50}Ca+^{176}Yb$

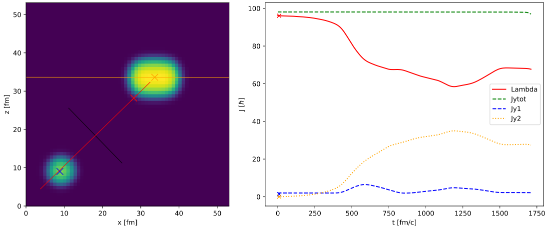

G. Scamps, Microscopic Study of Spin Transfer in Near-Barrier Nuclear Reactions, arXiv :2409.15018 (2024).

Thank you

TDHF

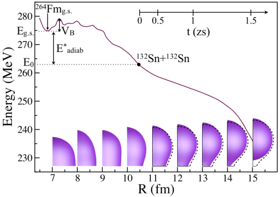

C. Simenel and A. S. Umar, Phys. Rev. C 89, 031601(R), 2014

TDHF+BCS

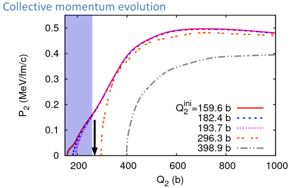

Y. Tanimura, D. Lacroix, and G. Scamps, PRC 92, 034601 (2015)

TDHFB

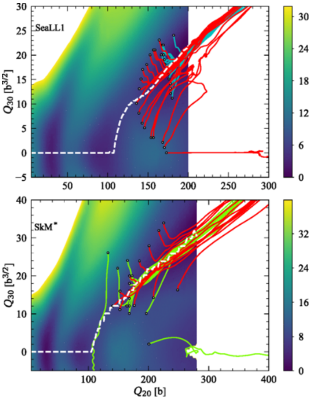

A. Bulgac, S. Jin, K. J. Roche, N. Schunck, and I. Stetcu Phys. Rev. C 100, 034615, 2019.

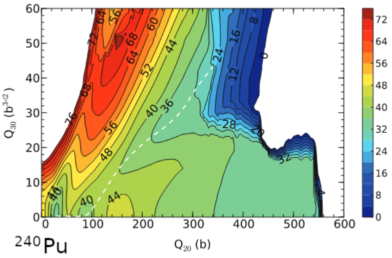

Rep. Prog. Phys. **79** (2016) 116301

Mainly two regimes before and after scission :
1) Overdamped motion, trajectory minimizing the energy
2) Fast separation, the asymmetry of the fission is frozen

Important

The fission properties are decided at scission